

ESD-TDR-65-28

ESD RECORD COPYRETURN TO
SCIENTIFIC & TECHNICAL INFORMATION DIVISION
(ESTI), BUILDING 1211

COPY NR. _____ OF _____ COPIES

ESTI PROCESSED☐ DDC TAB ☐ PROJ OFFICER☐ ACCESSION MASTER FILE☐ _____

DATE _____

ESTI CONTROL NR. **AL** 44759CY NR. 1 OF 1 CYS**Group Report****1965-3**

Experimental Observation
of the
Creeping Wave Phenomenon
in Backscatter
Using a Short Pulse Radar System

D. F. Sedivec
D. E. Foreman

14 January 1965

Prepared under Electronic Systems Division Contract AF 19 (628)-500 by

Lincoln Laboratory

MASSACHUSETTS INSTITUTE OF TECHNOLOGY

Lexington, Massachusetts



44759

The work reported in this document was performed jointly by General Dynamics, Fort Worth, Texas and Lincoln Laboratory, a center for research operated by Massachusetts Institute of Technology, with the support of the U.S. Air Force under Contract AF 19(628)-500.

MASSACHUSETTS INSTITUTE OF TECHNOLOGY
LINCOLN LABORATORY

EXPERIMENTAL OBSERVATION
OF THE CREEPING WAVE PHENOMENON IN BACKSCATTER
USING A SHORT PULSE RADAR SYSTEM

D. F. SEDIVEC

Group 21

D. E. FOREMAN

General Dynamics, Fort Worth, Texas

GROUP REPORT 1965-3

14 JANUARY 1965

LEXINGTON

MASSACHUSETTS

ABSTRACT

The short pulse radar return of two bodies was measured to determine the contribution of individual scattering elements to the overall cross section. Evidence is presented which appears to verify the existence of the creeping wave echo and shows it to be the predominant contribution to the return from these bodies at nose-on incidence.

Accepted for the Air Force
Stanley J. Wisniewski
Lt. Colonel, USAF
Chief, Lincoln Laboratory Office

TABLE OF CONTENTS

	ABSTRACT	11
I.	INTRODUCTION	1
II.	DESCRIPTION OF MEASURING SYSTEM	1
III.	DISCUSSION OF MEASUREMENTS	2
IV.	CONE-SPHERE	3
V.	SPHERE-CAPPED OGIVE	5
VI.	CONCLUSIONS	6
	ACKNOWLEDGEMENT	7
	REFERENCES	8

EXPERIMENTAL OBSERVATION OF THE CREEPING WAVE PHENOMENON IN BACKSCATTER USING A SHORT PULSE RADAR SYSTEM

Donald E. Foreman*, Darrel F. Sedivec

I. INTRODUCTION

Radar backscattering from a conductive cone-sphere has been treated by many, including Pannell, Rheinstein and Smith.¹ Their report discusses theoretical and measured backscattering data for a series of cone-spheres of various sphere radius-to-wavelength ratios. For the "nose-on" region (aspect angles near zero) the backscattering that does occur is believed to arise from three mechanisms:

- (1) Tip Scattering:- Diffraction by the pointed nose of the body; this would be the only contribution present for a cone of infinite length.
- (2) Traveling Waves:- Reflections of surface waves by surface derivative discontinuities; e.g., a finite right circular cone would show a gross effect because of the edge at its base.
- (3) Creeping Waves:- Radiation from surface waves which may be thought of as traveling around the rear (or shadowed region) and radiating back toward the illuminating source.

In cooperation with M.I.T. Lincoln Laboratory, short pulse radar backscatter experiments were conducted at General Dynamics, Fort Worth, Texas (GD/FW) on a cone-sphere, Fig. 1, and a sphere-capped ogive, Fig. 2. The purpose of these measurements was to verify the existence of the creeping wave return and to correlate its amplitude with the theoretical predictions presented in the report cited above.

II. DESCRIPTION OF MEASURING SYSTEM

The GD/FW S-Band (2Gc) short-pulse radar system was used in making the measurements. High range resolution (typically less than 1 foot) is

*Sr. Aerosystems Engineer, General Dynamics, Fort Worth, Texas.

obtained by transmitting an RF pulse which is very short, even with respect to the target dimensions; consequently, individual scattering points can be located and their relative amplitudes compared.

The peak power of the transmitted pulse is approximately one kilowatt and its width is typically less than 1 nanosecond at the half-power points.

The antenna system consists of two 6-foot diameter parabolic antennas with horn feeds. The gain of each antenna is greater than 25db. The return signals are amplified through a broad-band chain of traveling-wave tubes and displayed on a sampling oscilloscope. A precise variable attenuator is used for amplitude comparison. Over-all amplitude measurement accuracy is better than ± 1.5 db. Quasi-monostatic (less than 7° bistatic angle) backscattering measurements were made at a range of 125 feet with model and antenna systems both 15 feet above the ground. Backscatter from the rotator assembly was minimized by a tilted barrier (RAM) covered with radar absorber, and located approximately 25 feet in front of the rotator. The short pulse technique provides exceptionally good range discrimination with respect to both clutter returns and the return pulse carried by the ground reflected wave. Measurements were made with the models mounted on a small diameter styrofoam column. The background level was significantly below the amplitudes of concern at all aspect angles of interest. Optical instruments were used to align the axis of the models in the plane of incidence. Data were taken for both HH* and VV† polarizations at a sequence of aspect angles.

III. DISCUSSION OF MEASUREMENTS

The system was first tested with a vertically mounted styrofoam column of relatively high cross section. It can be seen in Fig. 3 that there are approximately 16.5 small divisions between radar pulse centers (column interfaces), 1 small division being equivalent to 1.2 inches. This is based on a radar echo delay of 1 nanosecond (large division) being equivalent to a range increment of 5.9 inches. Therefore, the column's

* Antennas horizontally polarized.

† Antennas vertically polarized.

radar diameter was 19.8 inches. The actual diameter was 19.7 inches.

IV. CONE-SPHERE

1. No External Markers

Both HH and VV short pulse measurements were made at aspect angles of 0° , 170° , 180° , and 190° . The data for HH are illustrated in Fig. 5, and for VV in Fig. 4. Referring to the 0° and 180° aspect angles for both polarizations, one predominant return can be seen to exist.

Because of body symmetry, we can assume the 180° returns to be caused by the specular return of the sphere. The backscatter cross section of a sphere of this size was computed* to be $-26.1 \text{ dbsm}^\dagger$. The backscatter patterns of Figs. 6 and 7 (obtained effectively at CW) show the measured specular return to be within $1/2 \text{ db}$ of the computed value for both polarizations.

Examination of both the short pulse and the conventional data at 0° and 180° aspect will show the nose-on and specular return levels to be approximately equal in amplitude. At 0° the predominant return is contributed by reflection of the traveling wave from the joint between cone and sphere, by the creeping wave, or both. It will be shown experimentally in 2. below that this return is apparently due only to the creeping wave. Conventional long pulse data (200 nanoseconds) as shown in Fig. 6 exhibit large amplitude perturbations in the vicinity of 180° . Examination of Fig. 6 shows a return significantly larger than specular at 170° and 190° as do the short pulse data in Fig. 5. It will be further noted in Fig. 5 that at 180° there is no observable return from the tip.

The short pulse data for VV polarization as shown in Fig. 4 illustrate the absence of any tip return as observed in HH polarization at 170° and 190° , since only one pulse was noted. "Conventional" (long pulse) data in Fig. 7 reveal no large amplitude perturbations in the vicinity of 180° and show the amplitude to be very near that of the calculated backscatter for the sphere. It will be further noted that the short pulse returns for

*

From Rheinsteins table.

$^\dagger \text{ dbsm}$ = decibels referred to one square meter.

VV polarization at 170°, 180°, and 190° aspect angles are of approximately equal amplitudes as are those of the conventional long pulse at these angles.

2. External Marker 18 Inches from Transition Region

The objective of this short pulse measurement was to verify that the backscattered energy observed for nose-on incidence for both HH and VV polarizations was apparently due to a creeping wave and not to reflections from the transition region. To show this, an external marker was placed on the surface of the model to establish accurately the positions of the transition region and of the creeping wave return. The external marker (a 1/2 inch square flat metal plate) was located 18 inches forward of the sphere-cone joint as shown in Fig. 8.

Figure 9 illustrates schematically the incident, reflected and creeping waves. Since the creeping wave is an apparent "slow" wave (traveling at a velocity less than the speed of light), its true path length will be greater than that surface distance πr . Van DeHulst² gives an expression which enables us to determine the effective sphere radius, r' of the sphere-cone (Fig. 9) for such a case:

$$r' = r (1 + 0.403 x^{-2/3}) \text{ where } x = 2\pi r/\lambda.$$

$$\text{for } \lambda = 5.901 \text{ in.}$$

$$\text{we find } r' = 1.415 \text{ in.}$$

$$\text{and } \pi r' = 4.444 \text{ in.}$$

Referring to Fig. 9, the two way radar distance R_2 , will be:

$$\begin{aligned} R_2 &= (18 + 4.444 + 18)/2 \text{ in.} \\ &= 20.222 \text{ in.} \end{aligned}$$

From the data in Fig. 10 the estimated separation between the return pulse centers is $19.9 \pm .6$ inches which is in good agreement with the theoretical value R_2 . Therefore, it is believed that the primary source of backscattering at nose-on is due to the creeping wave around the body. From Fig. 11 the creeping wave return is estimated to be -12db λ^2 for a/λ of 0.174. Although

Fig. 11 pertains to a sphere-cone whose half-angle is 15° , the creeping wave amplitude is not a function of the cone angle, but only of the sphere radius-to-wavelength ratio. Therefore, the creeping wave return should be -28.4dbsm or 2.3db less than the specular sphere return (-26.1dbsm measured at 180° with both conventional and short pulse techniques). Close inspection of the short pulse returns obtained at 0° and 180° for VV and HH polarizations does show the specular return to be slightly larger than the creeping wave return. That is, the 180° return pulse is somewhat larger than the 0° return pulse.

Short pulse data for 170° and 190° for HH and VV polarizations are also shown in Figs. 5 and 4. For the case of HH polarization at 170° and 190° , two return pulses are observed. The pulse on the left is due to the specular backscattering from the sphere and the pulse on the right is shown to be the tip surface wave return. Noting that 10db of system attenuation had been added for the HH data, it can be seen that the amplitude of the tip return is more than 10db above that of the specular (smaller) return from the sphere. It appears that the significant source of backscattering for HH polarization at 170° and 190° is due to a wave launched back toward the illuminating source from the tip discontinuity.

V. SPHERE-CAPPED OGIVE

Short pulse measurements were conducted on this body which is depicted in Fig. 2; the results are shown in Fig. 12. Data were obtained for both HH and VV polarizations at 0° and 180° aspect angles. External markers were employed for positive scatterer location.

Data for HH polarization are shown in "A", "B", and "C", of Fig. 12. Photograph "A" illustrates two return pulses at 0° where the pulse on the left is from the nose tip marker and the other pulse is from the creeping wave return. Photograph "B" illustrates three return pulses at 0° where the first and second pulse on the left side are returns from the nose tip and transition region markers respectively, and the remaining pulse on the right is apparently from the creeping wave return. From the dimensions of

the model shown in Fig. 2 the creeping wave return should be delayed by more than 13 inches in radar range or 1.14 large divisions with respect to the transition marker return in photograph "B". Photograph "B" gives good evidence that the significant scattering at 0° is due to the creeping wave. Photograph "C" shows a single return pulse for 180° which is due to the specular sphere return. The computed specular sphere return amplitude is -8.3dbsm. Noting that 20db of attenuation was used for "C", it can be seen by comparing the creeping wave return in either "A" or "B" to the sphere return in "C" that the creeping wave is approximately 20db less than the specular sphere return. From Fig. 11, the creeping wave amplitude (sphere radius-to-wavelength ratio of 1.5) is found to be -29.9dbsm which is 21.6db below the specular sphere return. Therefore, the measured and theoretical values for the amplitude of the creeping wave at nose-on are in close agreement.

Data for VV polarization are shown in "D" and "E" for 0° and 180° aspect angles respectively. Data at 0° again illustrate the creeping wave to be the only significant return. Photograph "E" shows the specular sphere return on the left and a return from the tip marker (which is now in the shadow zone of the sphere).

VI. CONCLUSIONS

The simple shape of both bodies, together with the high resolution capability of the short pulse radar, makes it relatively easy to identify the three individual scattering mechanisms. Short pulse amplitude comparisons between the specular returns of the spherical ends of both bodies and their respective creeping waves are in good agreement with the theoretical values¹. Additionally, the conventional long pulse amplitude data are also in good agreement when compared to the short pulse amplitude measurements for the cone-sphere at the aspect angles measured.

Correlation of measurements made by both radars substantiates the creeping wave data¹ and gives good evidence for the existence of creeping waves.

DFS/DEF:pma

ACKNOWLEDGEMENT

The authors wish to express their appreciation to B. Falk and J. Murchison of General Dynamics, Fort Worth, Texas, and P. C. Fritsch and J. D. Rheinstein of M.I.T. Lincoln Laboratory for their technical assistance in the preparation of this report.

REFERENCES

1. J. H. Pannell, J. Rheinstein, A. F. Smith, "Radar Scattering from a Conducting Cone-Sphere," Technical Report 349, Lincoln Laboratory, M.I.T. (2 March 1964).
2. Van DeHulst, Light-Scattering by Small Particles, (John Wiley and Sons, 1957).

3-21-5949

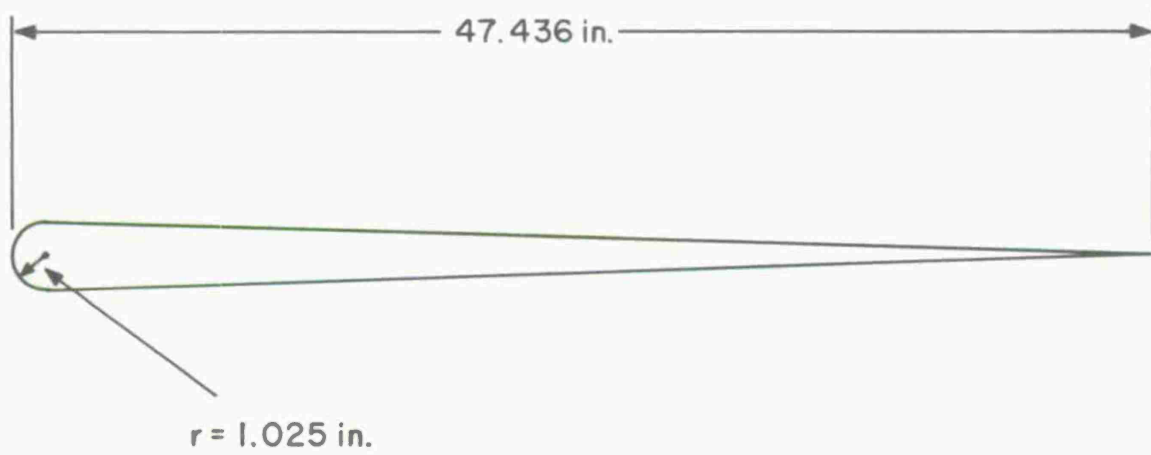


Fig. 1. Cone-Sphere.

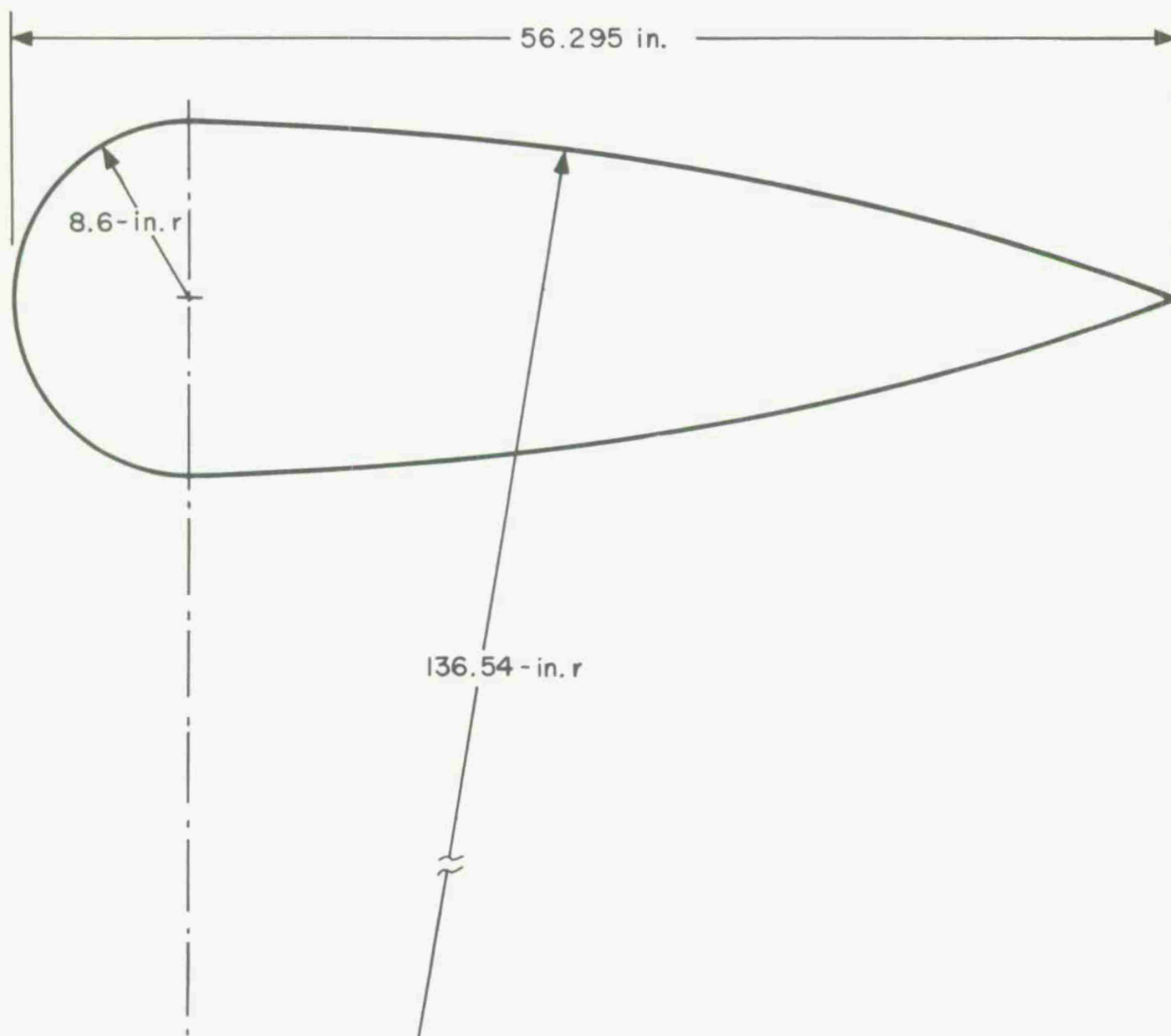
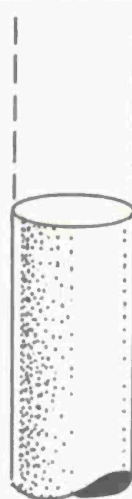
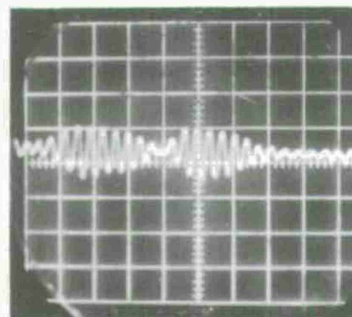


Fig. 2. Sphere-Capped Ogive.

-21-5951



STYROFOAM COLUMN
(of relatively high cross section)

Fig. 3. Styrofoam Column.

SHORT PULSE MEASUREMENTS OF METAL CONE-SPHERE

VERTICAL POLARIZATION (VV)

HORIZONTAL SCALE = 1 NANOSECOND / DIV (5.9 in.)

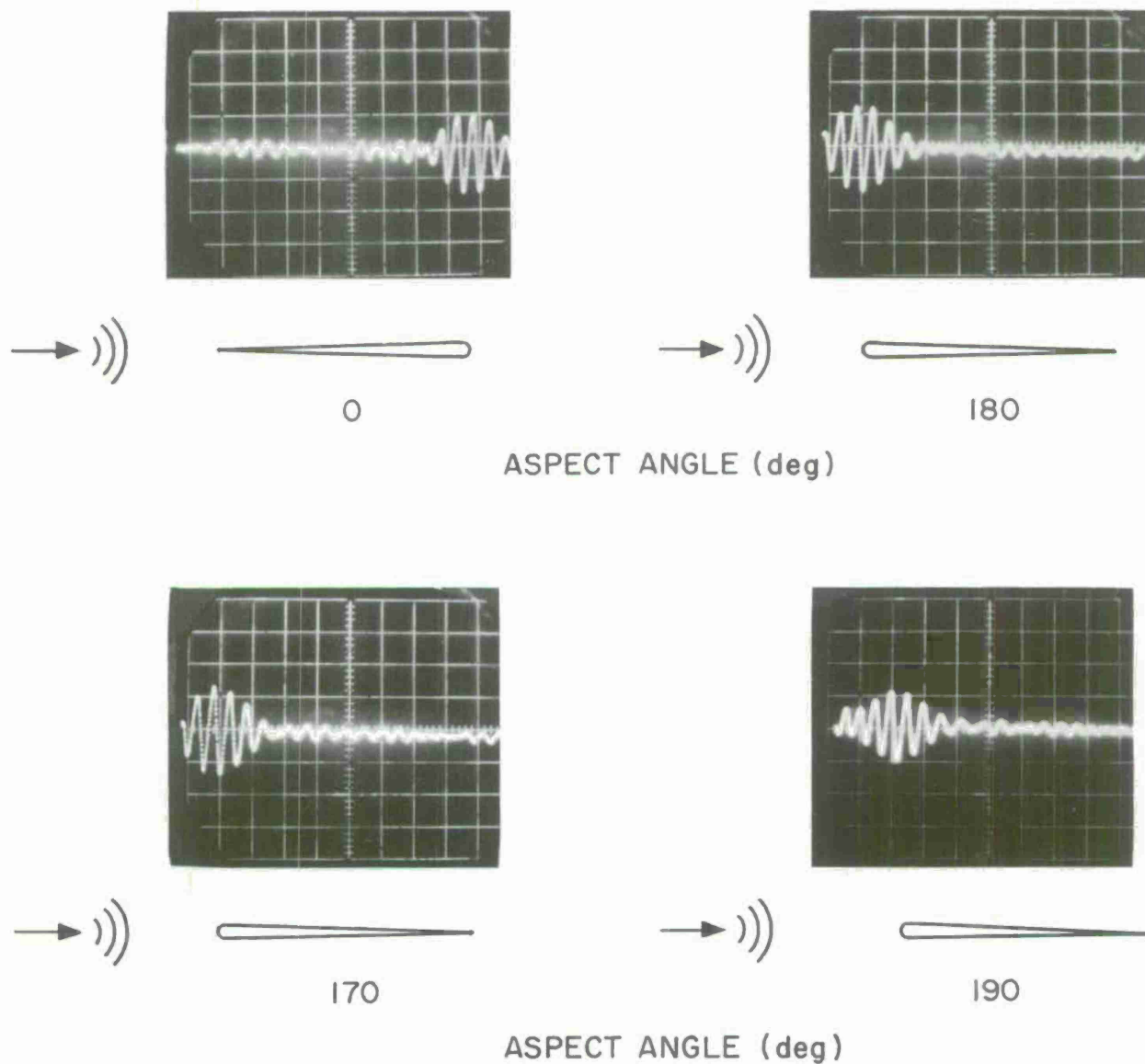


Fig. 4. Short Pulse Measurements of Metal Cone-Sphere.

SHORT PULSE MEASUREMENTS OF METAL CONE-SPHERE

HORIZONTAL POLARIZATION (HH)

HORIZONTAL SCALE = 1 NANOSECOND / DIV (5.9 in)

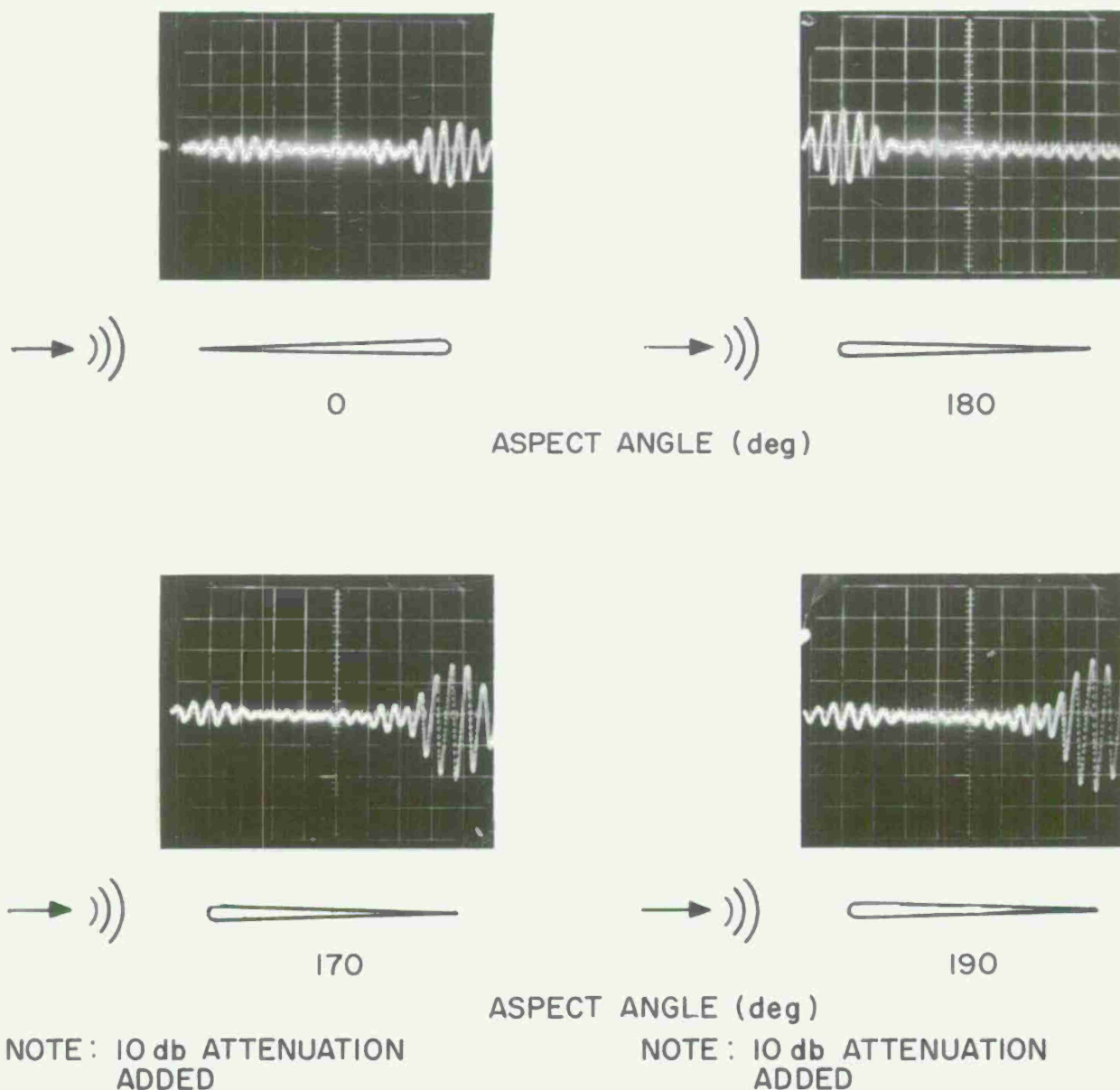


Fig. 5. Short-Pulse Measurements of Metal Cone-Sphere.

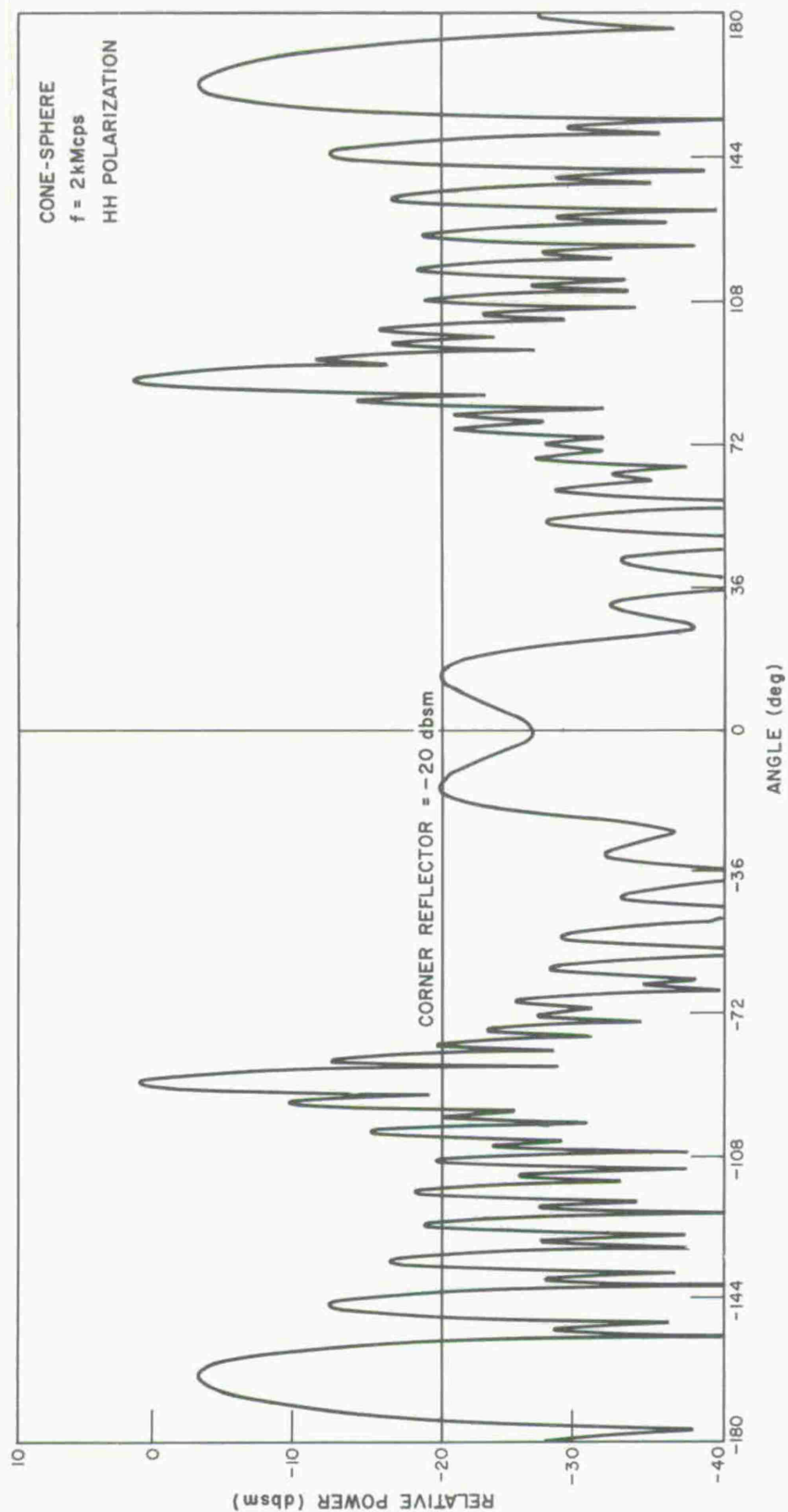


Fig. 6. Metal Cone-Sphere.

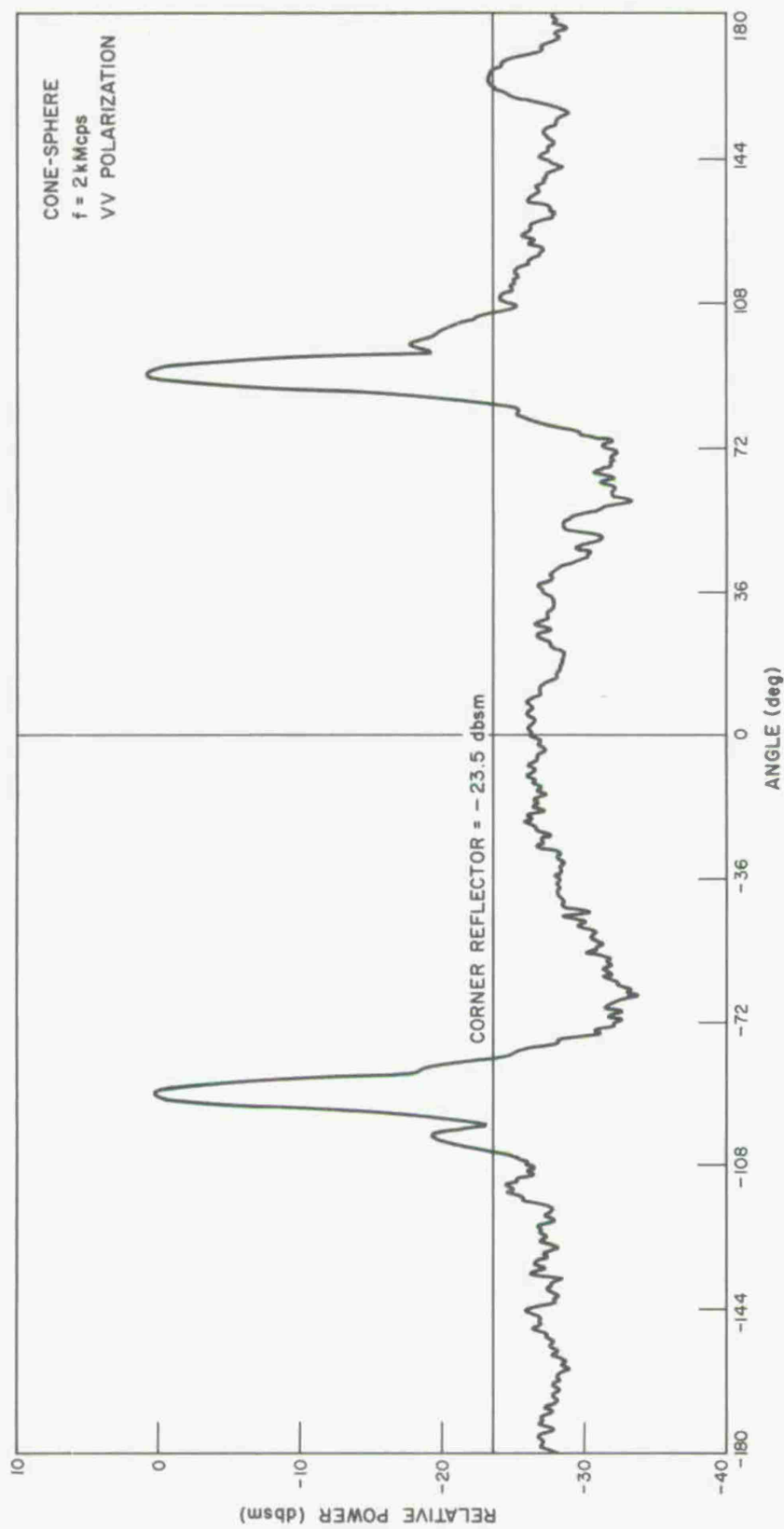


Fig. 7. Metal Cone-Sphere.

3-21-5956

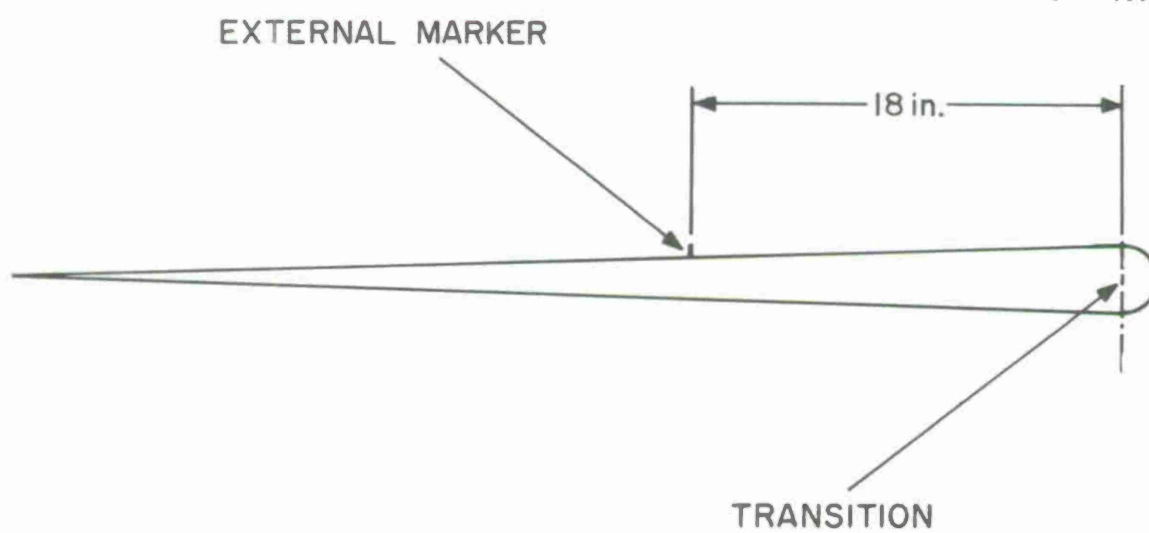


Fig. 8. Cone-Sphere.

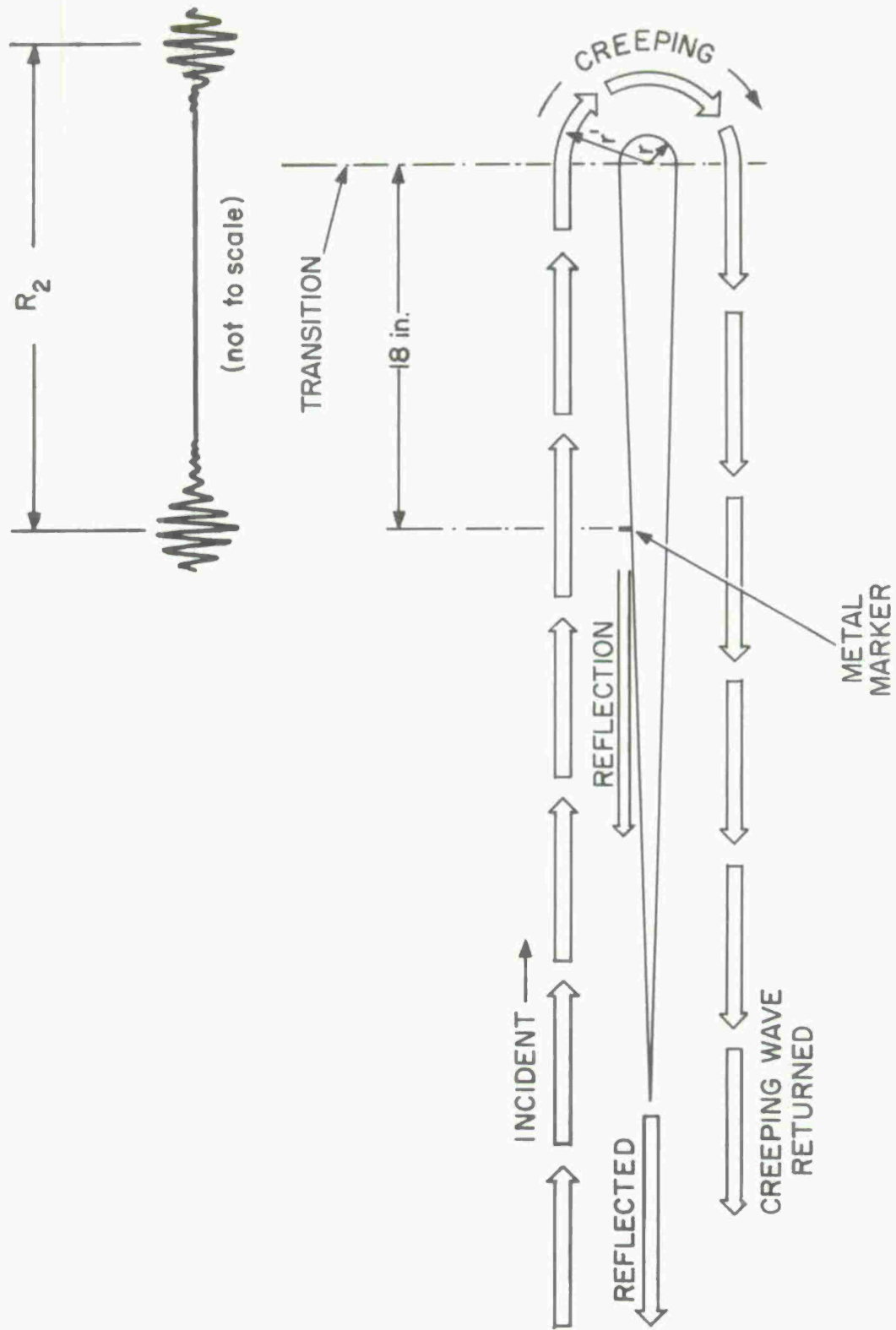
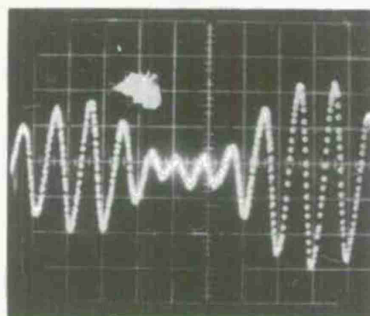


Fig. 9. Cone-Sphere.

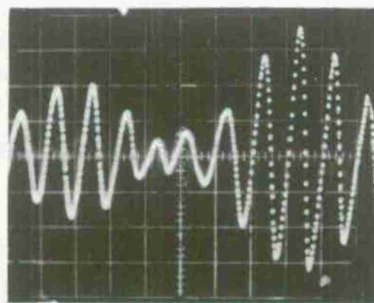
SHORT PULSE MEASUREMENTS OF METAL CONE-SPHERE
HORIZONTAL POLARIZATION (HH)



ASPECT ANGLE = 0 HORIZONTAL SCALE = 0.5 NANOSECOND / DIV (2.95 in.)

NOTE: AMPLITUDE SCALING CHANGED WITH RESPECT
TO OTHER PHOTOS FOR BOTH POLARIZATIONS

VERTICAL POLARIZATION (VV)



ASPECT ANGLE = 0 HORIZONTAL SCALE = 0.5 NANOSECOND / DIV (2.95 in.)

Fig. 10. Short Pulse Measurements of Metal
Cone-Sphere.

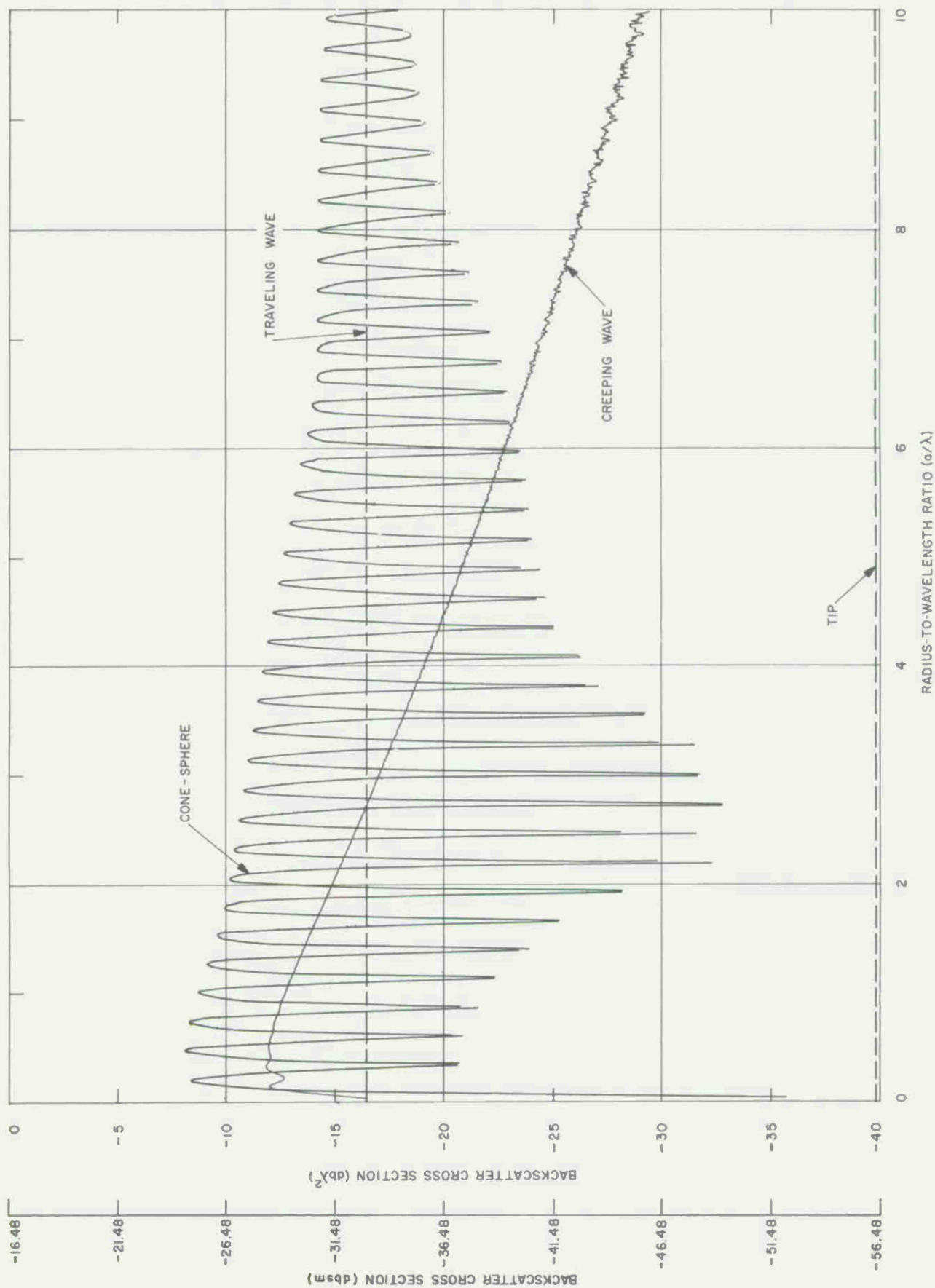
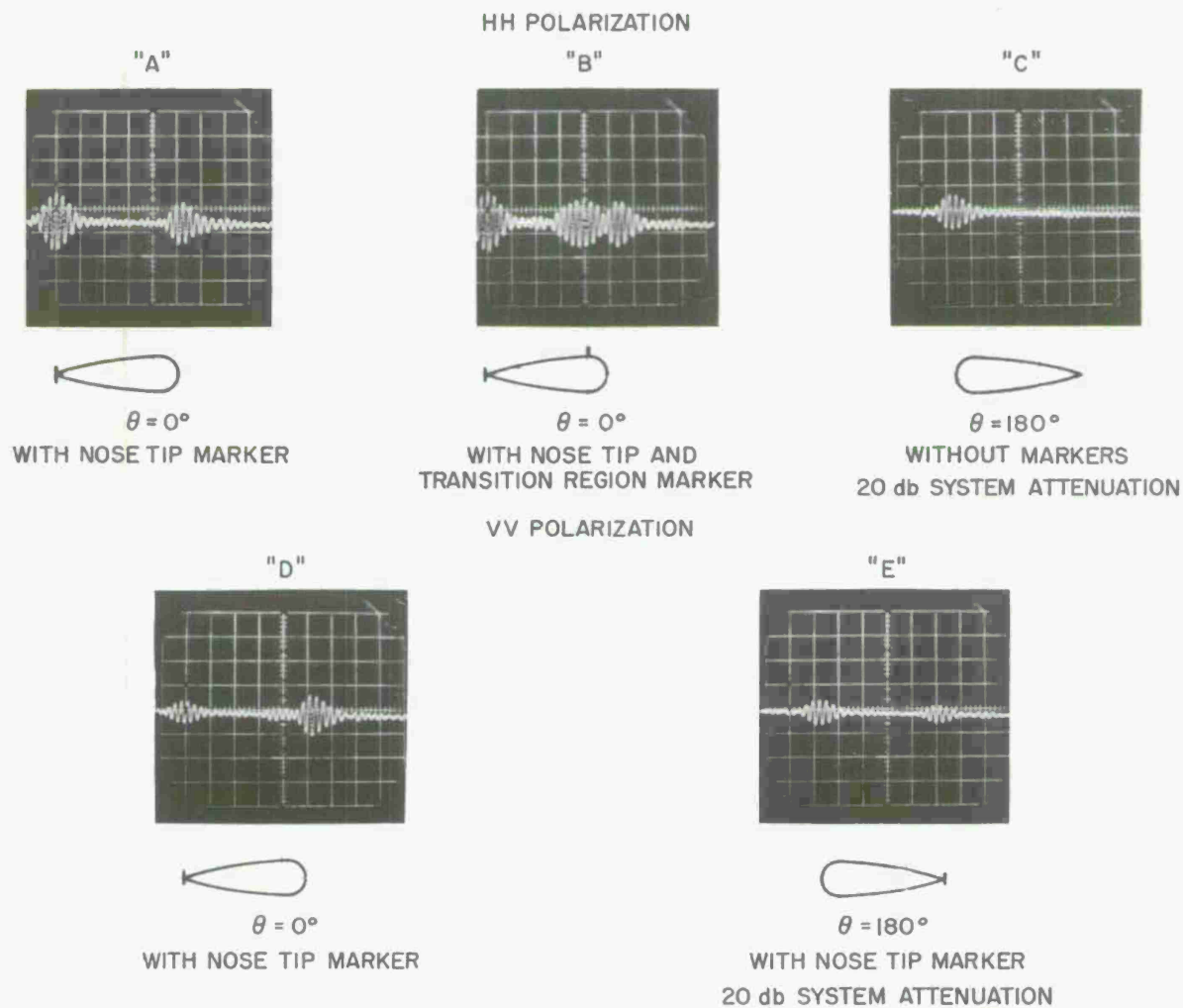


Fig. 11. Predicted Nose-On Backscatter Cross Section of a 15° Half-Angle Cone-Sphere.



HORIZONTAL TIME SCALE FOR ALL DATA = 11.8 in/LARGE DIVISION

Fig. 12. Short Pulse Data of Sphere-Capped Ogive.

DISTRIBUTION LIST

Director's Office

C. R. Wieser
D. E. Dustin

Division 2

F. C. Frick

Division 3

M. A. Herlin
J. Ruze

Division 4

J. Freedman
H. J. Pratt, Jr.

Group 21

O. V. Fortier
P. C. Fritsch
J. H. Halberstein
P. J. Harris
H. L. Kasnitz
D. F. Sedivec
G. M. Shannon
C. W. Uskavitch
L. C. Wilber

Group 22

J. Beckman
R. J. Bergemann

Group 22 (Cont'd)

A. J. Bogush
E. L. Eaton
W. Z. Lemnios
V. A. Nedzel
J. H. Pannell
E. W. Pike
J. Rheinstein
J. Salerno
A. F. Smith
W. I. Wells
A. J. Yakutis

Group 61

M. L. Rosenthal

Major H. C. Marlow
RATSCAT Site
Holloman AFB, New Mexico

D. A. Sherman
AVCO Corporation
Wilmington, Massachusetts

General Dynamics/Ft. Worth
Fort Worth, Texas

B. Falk (2)
D. E. Foreman (4)
B. R. Greene (2)
L. E. Heizer (1)
J. M. Murchison (2)
C. H. VanHoozer (3)

Printed by
United States Air Force
L. G. Hanscom Field
Bedford, Massachusetts

